Robot Swinging Using van der Pol Nonlinear Oscillators

Paschalis Veskos and Yiannis Demiris
Department of Electrical and Electronic Engineering
Imperial College London, SW7 2BT
{paschalis.Veskos, y.Demiris}@imperial.ac.uk
http://www.iis.ee.ic.ac.uk/yiannis

***Abstract*— In this study, we investigated the use of van der Pol oscillators in a 2-dof embodied robotic platform for a swinging task. The oscillator controlled the hip and knee joints of the robot and was capable of generating waveforms with the correct frequency and phase so as to entrain with the mechanical system.**

***Index Terms*— Biologically-inspired robotics, van der Pol oscillators, robotic swinging.**

I. Introduction

NONLINEAR differential equations have been used in robotics as central pattern generators (CPGs) for a multitude of tasks such as robot swinging [1], arm motion [2] and locomotion [3-5], both in simulation and robotic experiments. CPGs have become increasingly popular as they provide biologically-inspired, robust and adaptive motion.

With the use of CPGs in robot swinging, an interesting range of rhythmical behaviours can be explored. Thus, what might seem as an uncomplicated task offers the right amount of complexity to investigate and make comparisons with theoretical findings and different oscillators, while at the same time maintaining a controlled experimental environment.

In this paper, we extend the experimental results of [1] for robotic swinging to the van der Pol oscillator. The van der Pol oscillator [6] was chosen for the smaller number of parameters requiring tuning, robustness (Matsuoka is a near-harmonic oscillator that does not feature an asymptotically stable limit cycle) and straightforward computational implementation.

II. Experiments

A. Experimental Setup

The robot is held from a horizontal bar like a pendulum so that it can swing freely about it. A coloured marker is placed on the robot so that a webcam viewing the setup from the side can track the marker's position. The x coordinate of this marker is then used as feedback for the neural oscillator. In this study, only the hip and knee joints were actuated, while all others on the robot were held stiff. This way the system can be viewed as an underactuated triple pendulum with the top joint being free while the bottom two joints are totally forced to the output of the nonlinear oscillator. The experimental setup and an equivalent representation are shown in Fig. 1. The equivalent representation is only shown for clarity and was not used as a model of the system.

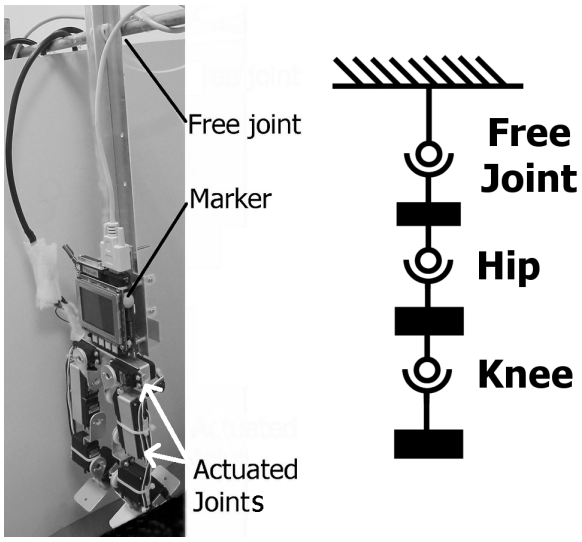

Fig. 1. The experimental setup and equivalent representation.

B. Nonlinear oscillator

The equations of the van der Pol oscillator, as used in our experiments, are:

$$\ddot{x}_{hip} + \mu\left(x_{hip}^2 - 1\right)\cdot \dot{x}_{hip} + \omega^2 x_{hip} = G_{in}\cdot fb + G_{hip-knee}\cdot x_{knee} \quad (1)$$

$$\ddot{x}_{knee} + \mu\left(x_{knee}^2 - 1\right)\cdot \dot{x}_{knee} + \omega^2 x_{knee} = G_{in}\cdot fb + G_{knee-hip}\cdot x_{hip} \quad (2)$$

where $\mu \geq 0$ is a parameter controlling the damping term, ω is the natural frequency of the oscillator, fb represents the feedback from the vision system, G_{in} is the feedback gain, while $G_{hip-knee}$ and $G_{knee-hip}$ are the cross-coupling term

gains. The final output given to the position-controlled motors activating the joints, is:

$$\theta_i = G_{out} \cdot sign(\dot{x}_i), \quad i = \{hip, knee\} \quad (3)$$

where G_{out} is the output gain.

Using the derivative of the equation's solution to generate the motor command has the effect of removing any DC components from the oscillator signal; taking the sign of this result generates a binary command for full joint extension or contraction (Fig. 2).

This is necessary for the low bandwidth motors that we use and also avoids the need for signal normalisation: unlike other nonlinear oscillators, the van der Pol's output varies in amplitude, dependant on the amplitude of its inputs [7]. We thus convert the periodic oscillator signal to a pulse-width modulated square wave retaining frequency information.

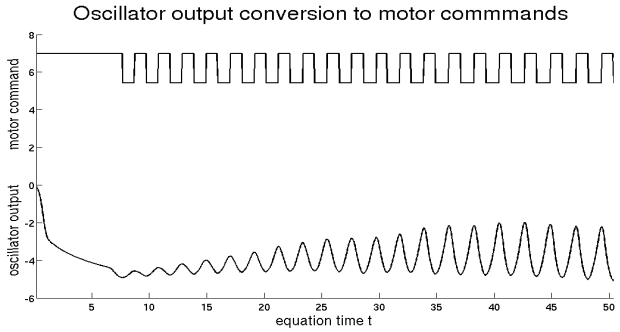

Fig. 2. Example oscillator output (e.g. x_{hip}, bottom waveform) and corresponding motor commands (θ, top waveform). Note that the drift in the DC component of the oscillator output does not affect the motor command.

By altering the gains, a range of different behaviours can be realised. If the value of G_{in} is too low, then the oscillator does not entrain to the feedback signal. Likewise, G_{out} has to be sufficiently high to 'excite' the mechanical system, yet given the low actuator bandwidth not so high as to make the distance the joints have to move excessively large. The gains affecting the cross-coupling terms control the influence each oscillator has on its counterpart. If they are not equal to each other, a phase difference between the two oscillators is introduced. To avoid this suboptimal behaviour, they were kept equal throughout this study.

Unless mentioned otherwise, the following values were used throughout the study: $\mu = 1.00$, $\omega^2 = 1.00$, $G_{in} = 0.143$, $G_{hip-knee} = G_{knee-hip} = 0.500$ and $G_{out} = 0.784$. The initial conditions given to the numerical integrators throughout this study were: $\{x_{hip}, \dot{x}_{hip}, x_{knee}, \dot{x}_{knee},\} = \{0.00, 0.00, 0.00, 0.00\}$.

III. Results

A. 1-DoF experimentation

Initially the system was only allowed to actuate the hip joint. As shown in Fig. 3, after a transient phase of increasing amplitude oscillations, the system settles into a stable oscillatory regime. The maximum amplitude reached was 163 units.

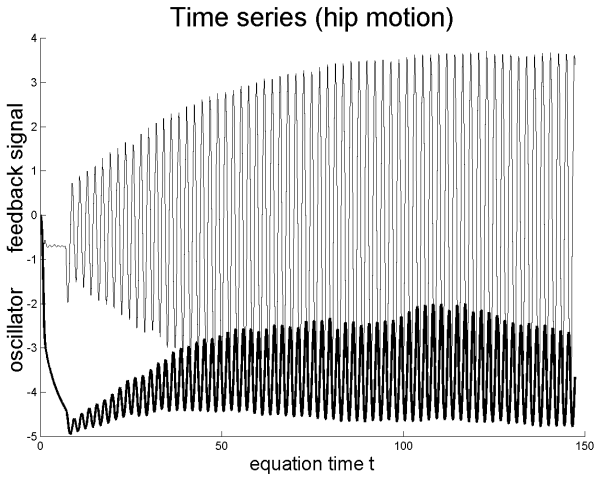

Fig. 3. The time series with the hip actuated. The top signal is fb and the bottom signal is oscillator output (x_{hip}).

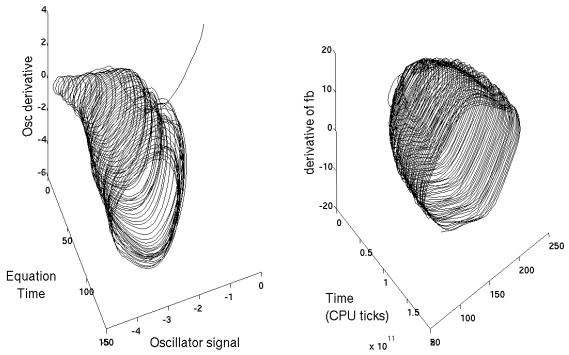

Fig. 4. Phase plots for the oscillator (left) and feedback signals (right) for a typical experimental run where the hip joint was actuated.

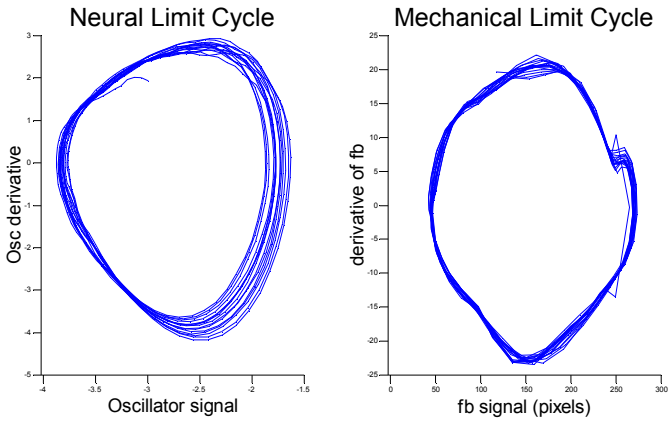

Fig. 5. Phase portraits of the steady state neural (left) and mechanical (right) system limit cycles.

The neural system entrains with the mechanical and is able to sustain stable oscillations, moving away from its initial conditions within the first half-period. A 2D projection (phase portrait) of the neural and mechanical limit cycles once the system has reached the steady-state is shown in Fig. 5.

Next, the system was run under the same setup, but with the output of the oscillator fed to the knee joints. Due to geometry and the fact that the motors move a smaller mass, the resultant oscillations were much smaller in amplitude (Fig. 6).

This way the feedback gain had to be significantly increased to 0.50 for entrainment to take place. The maximum oscillation amplitude attained in this setup was just 61 units. The mechanical system limit cycle contains multiple closed circular regions per iteration (knots), suggesting suboptimal behaviour.

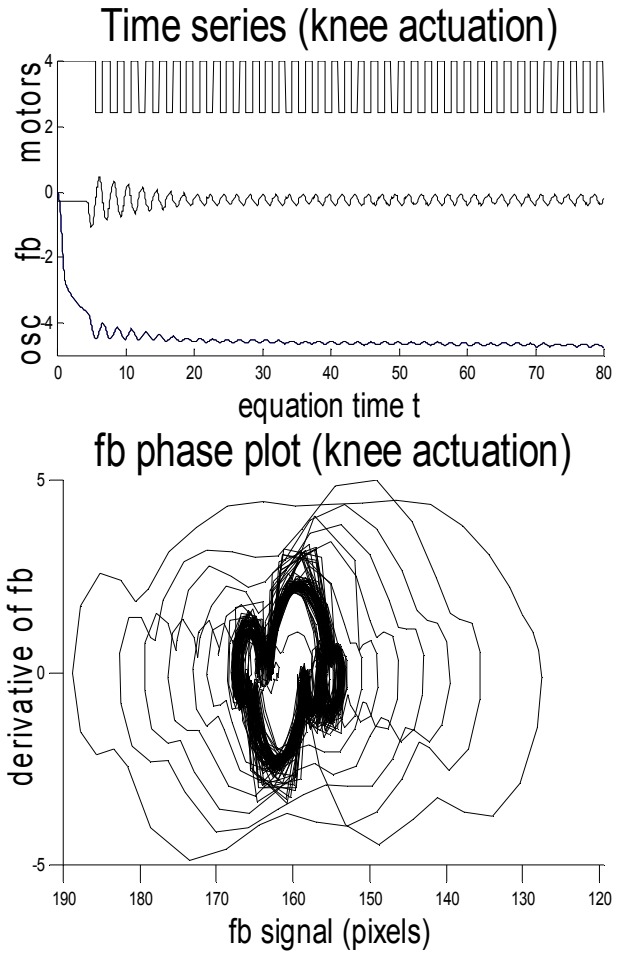

Fig. 6. Actuating the knee joints alone resulted in small amplitude oscillations. On the left, the time series is shown; from top to bottom, the signals are: knee servo command (θ), mechanical system position (fb) and oscillator output (xknee). On the right is a 2D projection of the fb limit cycle. The isolated external trajectories belong to the initial oscillations

B. *Independent 2-DoF experiments*

Subsequently, both joints were actuated at the same time. It was found that the system was able to perform much better in the 2-DoF configurations than the 1-DoF ones. Oscillations were more stable, of larger amplitude and the steady state was attained faster.

With the cross-coupling constants $G_{hip\text{-}knee}$ and $G_{knee\text{-}hip}$ set to 0, the two oscillators are only linked by means of the mechanical feedback signal. It was thus necessary to set the feedback gain parameter, $G_{in,}$, to a relatively high value (0.5) to allow sensory feedback to modulate the oscillator's output. This results in a stable oscillatory regime that attains maximal amplitude oscillations of 201 units (Fig. 7).

The regime is, however, prone to sporadic glitches during the transient phase, indicating that it is not totally stable. The time series and corresponding limit cycle for such a trial can be seen in Fig. 7. The glitches manifest themselves as single out-of-phase kicks, in addition to normal behaviour.

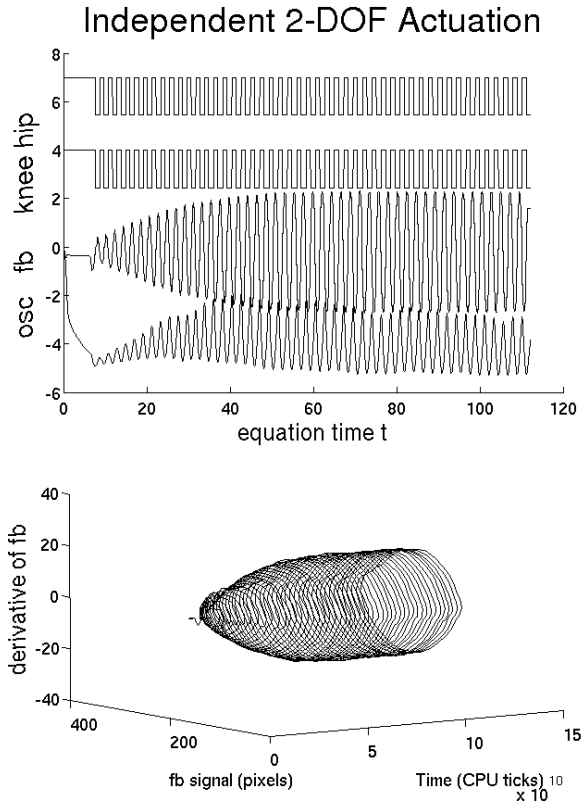

Fig. 7. Time series (left, top to bottom the signals shown are knee- and hip- servo commands, feedback signal and oscillator output) and mechanical phase plot (right) of the stable oscillatory regime obtained with cross-coupling disabled.

C. *Neural entrainment*

With the cross-coupling gains both set to 0.50, an explicit connection is made between the two oscillators. The output of each one is fed directly into the other, before exciting the motors. With this connection, the system finds a very stable oscillatory regime, even for low feedback gain values. Furthermore, the system reaches its steady-state faster and attains the largest maximal amplitude (206 units) among all experimental configurations. The time series and mechanical system phase plot can be seen in Fig. 8.

The corresponding phase plots for this experiment can be seen in Fig. 9. The mechanical limit cycle is now smoother and

varies less with time, but the neural system exhibits a low-frequency oscillation enveloping the normal behaviour.

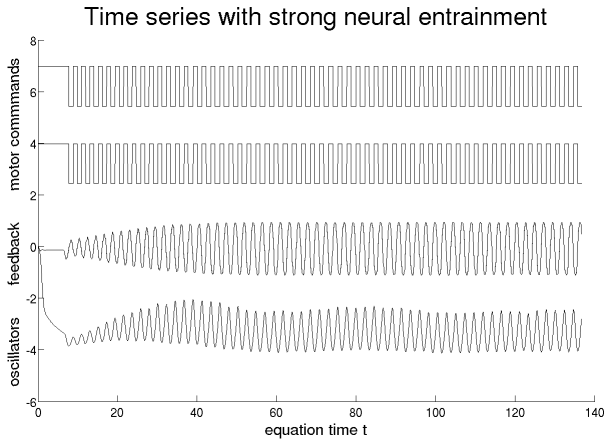

Fig. 8. Time series of the stable oscillatory regime obtained with cross-coupling enabled. Top to bottom the signals shown are knee- and hip- servo commands, feedback signal and oscillator output.

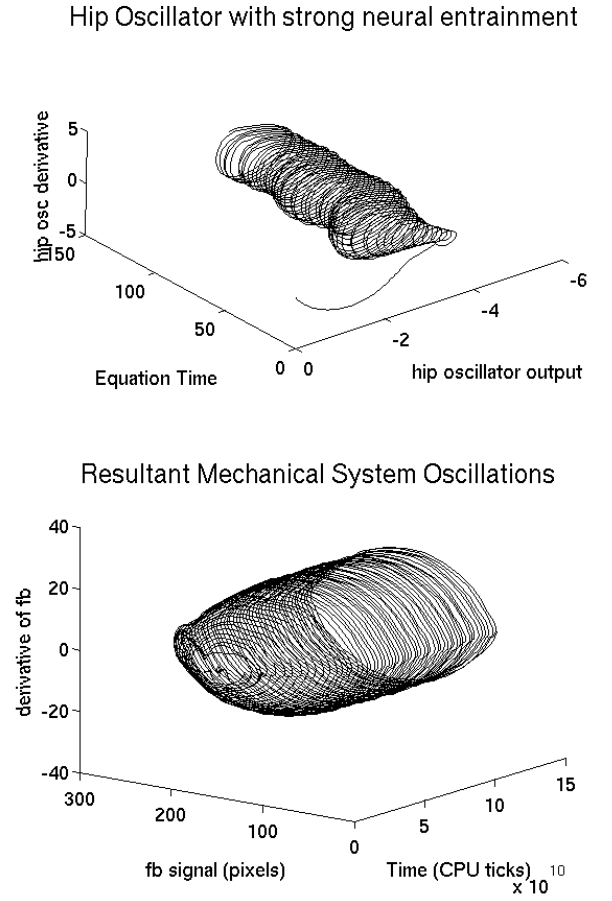

Fig. 9 Phase plots for the oscillator output (top) and mechanical feedback (bottom) signals in the presence of strong neural entrainment (cross-coupling gains both set to 0.50).

Provided that the feedback gain is high enough, the system can always reach a stable regime. The presence of neural entrainment acts as a stabiliser, removing glitches in the oscillator output and avoiding sudden transient behaviour. With the cross-coupling gains set to 0.25 the system achieves a maximum oscillation amplitude of 198 units and with the gains set to 0.10, 200 units.

IV. Conclusion

In the robot swinging task, the van der Pol oscillator successfully managed to achieve mechanical entrainment with either the proximal or distal degrees of freedom activated. While the latter exhibits suboptimal and volatile performance on its own, enabling both DoF results in a significant improvement of performance, without affecting stability.

In the presence of strong neural entrainment, the system reaches its maximal performance. This is in agreement with prior art [1, 3]. Furthermore, the strength of the connection between the oscillators seems to be directly related to the overall stability of the system, eliminating glitches in the oscillator outputs and reducing the duration of the transient phase.

Acknowledgment

The authors would like to thank the rest of the members of the BioART team, Anthony Dearden, Matthew Johnson, Bassam Khadouri and Gavin Simmons for their suggestions and constructive criticism.

References

[1] M. Lungarella and L. Berthouze, "On the Interplay Between Morphological, Neural, and Environmental Dynamics: A Robotic Case Study," *Adaptive Behavior*, vol. 10, pp. 223-242, 2002.

[2] M. M. Williamson, "Neural control of rhythmic arm movements," *Neural Networks*, vol. 11, pp. 1379-1394, 1998.

[3] G. Taga, "Self-organised control of bipedal locomotion by neural oscillators in unpredictable environment," *Biological Cybernetics*, vol. 65, pp. 147-159, 1991.

[4] T. Zielinska, "Coupled oscillators utilised as gait rhythm generators of a two-legged walking machine," *Biological Cybernetics*, vol. 74, pp. 263-273, 1996.

[5] M. A. Lewis, R. Etienne-Cummings, M. J. Hartmann, Z. R. Xu, and A. H. Cohen, "An in silico central pattern generator: silicon oscillator, coupling, entrainment, and physical computation," *Biological Cybernetics*, vol. 88, pp. 137-151, 2003.

[6] S. Strogatz, *Nonlinear Dynamics and Chaos: With Applications to Physics, Biology, Chemistry and Engineering*: Perseus Books Group, 2001.

[7] M. Williamson, "Robot Arm Control Exploiting Natural Dynamics," in *Department of Electrical Engineering and Computer Science*. Cambridge, Massachusetts: Massachusetts Institute of Technology, 1999.